

Integrated Pharmacognostic Characterization, Molecular Docking, Pharmacological Validation, And Advanced Drug Delivery System Development Of Novel Phytoconstituents Isolated From *Tinospora Cordifolia* For Neuroprotective Applications

N Ramasamy¹, Lalatendu Mohanty², Sumit Ghosh³, Ashok Thalkar⁴, Manu Jose⁵, Jaswinder Kaur⁶, Tanmay Ghosh⁷, Shilpi Prasad⁸, Nakul Gupta^{*9}

¹Professor, Department of Pharmacognosy, S. A. Raja Pharmacy College, Vadakkankulam, Tirunelveli, Tamilnadu, India

²Assistant Professor, Department of Pharmaceutical Science, HNB Garhwal University, Uttarakhand, India

³Assistant Professor, Department of Pharmaceutics, Pandaveswar School of Pharmacy, Pandaveswar, Paschim Bardhaman, West Bengal, India

⁴Assistant Professor, Department of Pharmacology, School of Pharmacy, Parul University, Vadodara, Gujarat, India

⁵Professor, Department of Pharmaceutical Chemistry, Nirmala College of Pharmacy Muvattupuzha Ernakulam, Kerala, India

⁶Assistant Professor, Medical lab Sciences, Chandigarh School of Business, Chandigarh Group of Colleges Jhanjeri, Mohali, Punjab, India

⁷Assistant Professor, Department of Microbiology, Dinabandhu Andrews College, Baishnabghata, South 24, Parganas, Kolkata, West Bengal, India

⁸Associate Professor, Department of Pharmaceutics, Siddhi Vinayaka Institute of Technology and Sciences, Bilaspur, Chhattisgarh, India

⁹Director and Professor, IIMT College of Pharmacy, Knowledge Park-III, Greater Noida, Uttar Pradesh, India

Abstract

Background: Neurodegenerative disorders, including Alzheimer's and Parkinson's diseases, represent a growing global health challenge characterized by oxidative stress, neuroinflammation, and protein misfolding. *Tinospora cordifolia*, a traditional Ayurvedic medicinal plant, has long been used for neurological disorders. This study aimed to integrate pharmacognostic characterization, molecular docking, in vitro and in vivo validation, and advanced drug delivery systems to evaluate its neuroprotective potential.

Methods: Authentic *T. cordifolia* stems were collected and subjected to pharmacognostic evaluation, physicochemical analysis, and phytochemical extraction. Major phytoconstituents were isolated and structurally elucidated using HPLC, NMR, and LC-MS/MS. Molecular docking was performed against targets including AChE, BChE, MAO-B, NMDA receptor, Tau protein, and β -amyloid. In vitro neuroprotective activity was assessed via antioxidant (DPPH, ABTS, FRAP), cholinesterase inhibition, and neuronal cell protection assays (SH-SY5Y, PC12). In vivo validation employed rodent models of neurodegeneration (scopolamine, AlCl₃, rotenone), assessing behavioral, biochemical, and histopathological endpoints. Nanocarrier formulations of lead compounds were developed and evaluated for size, zeta potential, entrapment efficiency, release kinetics, and BBB penetration.

Results: Pharmacognostic and phytochemical analyses confirmed the presence of bioactive alkaloids (berberine, magnoflorine, palmatine) and diterpenoid glycosides (tinosporaside). Molecular docking predicted strong binding to cholinesterases and amyloid targets, correlating with in vitro enzyme inhibition and antioxidant activity. In vivo studies demonstrated improved cognitive performance, restored oxidative markers, and preserved neuronal architecture in berberine- and magnoflorine-treated groups. Nanocarrier formulations enhanced brain delivery, sustained release, and pharmacokinetic profiles.

Conclusion: Phytoconstituents from *T. cordifolia* exhibit multi-target neuroprotective effects, which are significantly enhanced by nanocarrier delivery systems. These findings support their potential development as safe and effective therapeutic agents for neurodegenerative disorders.

Keywords: *Tinospora cordifolia*, neuroprotection, berberine, magnoflorine, molecular docking, nanocarrier, Alzheimer's disease, oxidative stress

1. INTRODUCTION

Neurodegenerative disorders such as Alzheimer's disease (AD), Parkinson's disease (PD), and related dementias represent a significant global health challenge. According to the World Health Organization, more than 55 million people worldwide are currently living with dementia, with nearly 10 million new cases reported annually (World Health Organization [WHO], 2023). Alzheimer's disease alone accounts for 60–70% of these cases, while Parkinson's disease is the fastest-growing neurological condition in prevalence and disability burden (Dorsey et al., 2018). The increasing life expectancy and aging populations worldwide are projected to accelerate the prevalence of these conditions, underscoring the urgent need for effective preventive and therapeutic strategies (GBD Neurology Collaborators, 2021).

The pathophysiology of neurodegenerative disorders is complex, involving multiple mechanisms such as oxidative stress, mitochondrial dysfunction, neuroinflammation, excitotoxicity, and protein misfolding. In Alzheimer's disease, for instance, abnormal accumulation of β -amyloid plaques and hyperphosphorylated tau tangles lead to synaptic dysfunction and neuronal loss (Querfurth & LaFerla, 2010). Parkinson's disease, on the other hand, is characterized by α -synuclein aggregation and dopaminergic neuronal degeneration, in which oxidative stress and neuroinflammation play central roles (Surmeier et al., 2017). Despite advances in drug development, most available therapies remain symptomatic, failing to address the multifactorial etiology or slow disease progression.

Herbal medicine has emerged as a promising complementary strategy due to its multi-targeted bioactive phytoconstituents. *Tinospora cordifolia* (Willd.) Miers ex Hook. f. & Thomson, commonly known as "Guduchi" or "Amrita," is a widely used medicinal plant in Ayurveda and traditional Indian medicine. It is revered for its Rasayana (rejuvenating) properties, particularly in promoting cognitive function, vitality, and resilience against aging-related decline (Patel & Mishra, 2012). Pharmacological studies have demonstrated that extracts and isolated compounds of *T. cordifolia* exhibit antioxidant, anti-inflammatory, immunomodulatory, and neuroprotective activities (Sarma et al., 2019; Upadhyay et al., 2010). These properties suggest that *T. cordifolia* may serve as a valuable candidate for developing novel neurotherapeutics. However, the therapeutic translation of herbal leads faces several challenges, including variability in phytochemical composition, lack of pharmacognostic standardization, incomplete mechanistic validation, and poor bioavailability of active compounds. Therefore, a multidisciplinary approach integrating pharmacognostic characterization, in silico molecular docking, in vitro and in vivo pharmacological validation, and advanced drug delivery system development is essential. Such an integrative strategy can ensure the identification of novel phytoconstituents, clarify their mechanisms of action, and enhance their therapeutic potential through optimized formulations.

Objectives of the study:

1. To conduct pharmacognostic and phytochemical characterization of *Tinospora cordifolia* extracts and isolated compounds.
2. To perform molecular docking and ADMET predictions of isolated phytoconstituents against key neurodegenerative targets.
3. To evaluate the in vitro antioxidant, enzyme inhibitory, and neuroprotective effects of candidate compounds.
4. To validate neuroprotective efficacy in vivo using established models of neurodegeneration.
5. To develop and characterize advanced drug delivery systems for enhancing brain bioavailability of lead phytoconstituents.

By combining pharmacognostic, computational, pharmacological, and formulation approaches, this study aims to provide comprehensive insights into the neuroprotective potential of *T. cordifolia*, facilitating its translational application in managing neurodegenerative disorders.

2. MATERIALS AND METHODS

2.1 Plant Material Collection and Authentication

Fresh stems of *Tinospora cordifolia* (Willd.) were collected from the medicinal plant garden of S. A. Raja Pharmacy College, Vadakkankulam, Tirunelveli, Tamil Nadu, India. The plant material was authenticated by a taxonomist in S. A. Raja Pharmacy College, and a voucher specimen was deposited in the departmental herbarium for future reference. The collected stems were thoroughly washed, shade-dried at room temperature (25 ± 2 °C), and coarsely powdered using a mechanical grinder before use (Kokate et al., 2010; WHO, 2011).

2.2 Pharmacognostic Characterization

2.2.1 Macroscopic and Microscopic Examination

Organoleptic characters (color, odor, taste, and texture) of the powdered *T. cordifolia* stems were noted. Microscopic evaluation was performed using free-hand sections stained with phloroglucinol and concentrated HCl to observe lignified elements such as xylem fibers and vessels. The powder microscopy included observations of diagnostic features like starch granules, fibers, parenchyma, and sclereids (Evans, 2009).

2.2.2 Physicochemical Constants

Standard physicochemical evaluations were carried out according to the guidelines of the World Health Organization and Indian Pharmacopoeia. These included determination of:

- Total ash value
- Acid-insoluble ash
- Water-soluble ash
- Alcohol-soluble extractive value
- Water-soluble extractive value

Each analysis was performed in triplicate, and results were expressed as mean \pm standard deviation (WHO, 2011; Khandelwal, 2012).

2.2.3 Fluorescence and Powder Analysis

Powdered drug samples were treated with different chemical reagents (1N NaOH, 1N HCl, concentrated H₂SO₄, iodine solution, etc.) and observed under visible light and UV light (254 nm and 366 nm) to record fluorescence characteristics. Powder microscopy was performed using a trinocular microscope, and diagnostic cellular structures were identified (Chaudhury & Sharma, 2014).

2.3 Phytochemical Extraction and Isolation

2.3.1 Extraction Procedure

Coarsely powdered stems (500 g) of *T. cordifolia* were subjected to successive solvent extraction in a Soxhlet apparatus using solvents of increasing polarity: hexane, ethyl acetate, methanol, and water. Each extraction was carried out for 48–72 hours until exhaustion of phytoconstituents was achieved. The extracts were filtered, concentrated under reduced pressure using a rotary evaporator at 40 °C, and stored at 4 °C in airtight containers (Harborne, 1998).

2.3.2 Fractionation and Isolation

The methanolic extract, found richest in secondary metabolites, was further fractionated using liquid–liquid partitioning into chloroform, ethyl acetate, and n-butanol fractions. Active fractions were subjected to column chromatography using silica gel (60–120 mesh) as stationary phase and eluted with gradient mixtures of solvents (e.g., hexane–ethyl acetate, chloroform–methanol). Fractions with similar TLC profiles (visualized under UV light and using spraying reagents such as vanillin–sulfuric acid) were pooled together. Pure compounds were further purified using preparative HPLC (C18 reverse-phase column, acetonitrile–water gradient system) (Mishra et al., 2014).

2.3.3 Structural Elucidation

The isolated phytoconstituents were structurally characterized using:

- UV-Visible spectroscopy for functional group transitions.
- Fourier Transform Infrared Spectroscopy (FTIR) for characteristic functional groups.
- Nuclear Magnetic Resonance (NMR, ¹H and ¹³C) for proton and carbon skeleton elucidation.

- Liquid Chromatography–Mass Spectrometry (LC-MS/MS) for molecular weight determination and fragmentation pattern analysis. Spectral data were compared with literature and reference standards for confirmation of compound identity (Silverstein et al., 2014).

2.4 Molecular Docking Studies

2.4.1 Target Protein Selection

Protein structures relevant to neurodegeneration were selected as molecular targets: acetylcholinesterase (AChE, PDB ID: 4EY7), butyrylcholinesterase (BChE, PDB ID: 4BDS), monoamine oxidase B (MAO-B, PDB ID: 2V5Z), N-methyl-D-aspartate (NMDA) receptor (PDB ID: 4PE5), tau protein (PDB ID: 5O3L), and β -amyloid fibrils (PDB ID: 2M4J). Crystal structures were retrieved from the Protein Data Bank (PDB). Water molecules and co-crystallized ligands were removed, and hydrogen atoms were added using AutoDock Tools 1.5.6 (Morris et al., 2009).

2.4.2 Ligand Preparation

Phytoconstituents isolated from *Tinospora cordifolia* were drawn in ChemDraw and converted into 3D conformers using Chem3D or MarvinSketch. Energy minimization was performed using the MMFF94 force field to obtain stable conformations. Ligands were then converted into PDBQT format for AutoDock Vina or prepared in Maestro for Schrödinger Glide (Trott & Olson, 2010; Friesner et al., 2004).

2.4.3 Docking Procedure

Docking simulations were conducted using AutoDock Vina and Schrödinger Glide to predict binding modes and affinities. The docking grid box was centered at the active site of each target protein, defined by co-crystallized ligand coordinates. Default docking parameters were applied, and the best docking poses were ranked according to binding affinity (kcal/mol) and hydrogen bonding/ π - π interactions with key residues.

2.4.4 Visualization and Analysis

Docking results were visualized using PyMOL and Discovery Studio Visualizer. 2D and 3D interaction plots were generated to identify hydrogen bonds, hydrophobic interactions, and π -stacking with catalytic residues.

2.4.5 ADMET and Drug-Likeness Prediction

Drug-likeness of the top-scoring phytoconstituents was evaluated using SwissADME (Daina et al., 2017) for Lipinski's rule of five, bioavailability, and pharmacokinetic predictions. Toxicity profiles, including hepatotoxicity, mutagenicity, and blood-brain barrier (BBB) penetration, were predicted using pkCSM (Pires et al., 2015).

2.5 In Vitro Neuroprotective Screening

2.5.1 Antioxidant Assays

• DPPH Radical Scavenging Assay

A 0.1 mM DPPH solution in methanol was prepared, and different concentrations of extracts/isolated compounds were added. After incubation for 30 minutes in the dark, absorbance was measured at 517 nm. Ascorbic acid was used as a positive control. Radical scavenging activity (%) was calculated (Brand-Williams et al., 1995).

• ABTS Radical Scavenging Assay

ABTS \bullet + was generated by mixing 7 mM ABTS with 2.45 mM potassium persulfate and incubating overnight. The solution was diluted to an absorbance of 0.70 ± 0.02 at 734 nm, and test samples were added. Trolox was used as standard (Re et al., 1999).

• Ferric Reducing Antioxidant Power (FRAP) Assay

The FRAP reagent (acetate buffer, TPTZ, FeCl_3) was prepared fresh. Test samples were added, incubated at 37 °C for 30 minutes, and absorbance measured at 593 nm. Results were expressed in $\mu\text{M Fe}^{2+}$ equivalents (Benzie & Strain, 1996).

2.5.2 Enzyme Inhibition Assays

• Acetylcholinesterase (AChE) Inhibition

The Ellman method was employed, using acetylthiocholine iodide as the substrate and DTNB (5,5'-dithiobis(2-nitrobenzoic acid)) as the chromogen. Inhibition was monitored spectrophotometrically at 412 nm. Donepezil served as a standard inhibitor (Ellman et al., 1961).

• Butyrylcholinesterase (BChE) Inhibition

Similar methodology was applied using butyrylthiocholine iodide as substrate. Galantamine was used as a standard inhibitor.

2.5.3 Neuroprotection Assays in Neuronal Cell Lines

- **Cell Culture**

Human neuroblastoma SH-SY5Y cells and rat pheochromocytoma PC12 cells were cultured in DMEM supplemented with 10% FBS, 1% penicillin–streptomycin at 37 °C under 5% CO₂.

- **Oxidative Stress Induction**

Cells were pretreated with test compounds followed by induction of oxidative stress using H₂O₂ (100–200 μM).

- **Cell Viability Assay (MTT Assay)**

MTT (0.5 mg/mL) was added to cells and incubated for 4 hours. The formazan crystals formed were dissolved in DMSO, and absorbance was measured at 570 nm.

- **Intracellular ROS Measurement**

ROS levels were measured using DCFH-DA (2',7'-dichlorofluorescein diacetate) fluorescent dye. Fluorescence intensity was detected using a microplate reader (Ex/Em: 485/530 nm).

- **Apoptosis and Neuroprotection Markers**

Hoechst 33342 staining and flow cytometry with Annexin V/PI were performed to evaluate apoptosis. Expression levels of neuroprotective markers (e.g., BDNF, caspase-3) were analyzed by Western blotting.

2.6 In Vivo Pharmacological Validation

2.6.1 Animal Model Selection

Healthy adult male Wistar rats (180–220 g) or Swiss albino mice (20–25 g) were obtained from the Central Animal House Facility of S. A. Raja Pharmacy College, Vadakkankulam, Tirunelveli, Tamilnadu, India. Animals were housed in polypropylene cages under controlled conditions (temperature 22 ± 2 °C, humidity 50–60%, 12 h light/dark cycle) with free access to standard pellet diet and water. All experimental protocols were approved by the Institutional Animal Ethics Committee (IAEC) and conducted in accordance with CPCSEA guidelines.

2.6.2 Induction of Neurodegeneration

Neurodegeneration was induced by the following models:

- **Scopolamine-induced amnesia:** Single intraperitoneal (i.p.) injection of scopolamine hydrobromide (1 mg/kg) to impair cholinergic neurotransmission (Klinkenberg & Blokland, 2010).

- **Aluminum chloride model:** Chronic administration of AlCl₃ (50 mg/kg, orally, 6 weeks) to induce Alzheimer-like pathology (Prakash & Kumar, 2014).

- **Rotenone model:** Subcutaneous administration of rotenone (2.5 mg/kg, daily for 21 days) to induce Parkinson-like neurodegeneration (Sherer et al., 2003).

Animals were divided into groups (n = 6) as follows: normal control, disease control, standard drug (donepezil or levodopa), and test groups treated with isolated phytoconstituents/nanoformulations.

2.6.3 Behavioral Assessments

- **Morris Water Maze (MWM):** Spatial learning and memory were assessed by recording escape latency time and time spent in the target quadrant during the probe trial (Vorhees & Williams, 2006).

- **Y-Maze Test:** Spontaneous alternation behavior was recorded to evaluate working memory performance (Maurice et al., 1994).

- **Open Field Test:** Locomotor activity, exploration, and anxiety-like behavior were recorded using video tracking software (Walsh & Cummins, 1976).

2.6.4 Biochemical Assays

After behavioral studies, animals were sacrificed, and brain homogenates were prepared for biochemical analysis:

- **Superoxide dismutase (SOD) activity** (Marklund & Marklund, 1974).

- **Catalase (CAT) activity** (Aebi, 1984).

- **Reduced glutathione (GSH) levels** (Ellman, 1959).

- **Malondialdehyde (MDA, lipid peroxidation index)** (Ohkawa et al., 1979).

- **Acetylcholinesterase (AChE) activity** using Ellman's method (Ellman et al., 1961).

2.6.5 Histopathology and Immunohistochemistry

Brain tissues (hippocampus and cortex) were fixed in 10% formalin, embedded in paraffin, sectioned, and stained with hematoxylin–eosin for general morphology. Congo red and thioflavin-S staining were used for

amyloid deposits. Immunohistochemical staining was performed for markers such as A β , phosphorylated tau, GFAP (astrocytes), and caspase-3 (apoptosis). Sections were analyzed under a light/fluorescence microscope, and digital images were recorded.

2.7 Advanced Drug Delivery System Development

2.7.1 Formulation of Nanocarriers

Lead phytoconstituents with promising *in silico* and *in vivo* neuroprotective potential were formulated into:

- **Polymeric nanoparticles** using nanoprecipitation (PLGA-based).
- **Nanoliposomes** via thin-film hydration method.
- **Nanogels** using natural polymers (chitosan, alginate).

Stabilizers such as poloxamers or lecithin were used to enhance stability (Patra et al., 2018).

2.7.2 Physicochemical Characterization

Formulations were characterized for:

- **Particle size, polydispersity index (PDI), and zeta potential** using dynamic light scattering (DLS).
- **Surface morphology** using scanning electron microscopy (SEM) and transmission electron microscopy (TEM).
- **Entrapment efficiency (EE%)** determined by centrifugation and spectrophotometric/LC-MS quantification.
- **In vitro release kinetics** studied in phosphate-buffered saline (PBS, pH 7.4) using dialysis bag method at 37 °C, analyzed via UV or HPLC (Dash et al., 2010).

2.7.3 In Vitro Blood–Brain Barrier (BBB) Permeation Studies

- **PAMPA-BBB assay:** Parallel artificial membrane permeation assay mimicking BBB lipid bilayers (Di et al., 2003).
- **Transwell model:** Co-culture of human brain endothelial cells (hCMEC/D3) and astrocytes used to assess trans-endothelial electrical resistance (TEER) and permeability of formulations (Cecchelli et al., 2007).

2.7.4 In Vivo Pharmacokinetics and Brain Distribution

Formulations were administered via oral/intravenous route to rats. Blood samples were collected at predetermined intervals, and plasma levels of phytoconstituents were quantified using LC-MS/MS. Brain tissue concentrations were determined by homogenization and extraction. Pharmacokinetic parameters (C_{max}, T_{max}, AUC, half-life, bioavailability) were calculated using non-compartmental analysis (Gao et al., 2017).

3. RESULTS

3.1 Pharmacognostic Data

3.1.1 Macroscopic and Microscopic Features

The stems of *Tinospora cordifolia* were cylindrical, 0.5–1.5 cm in diameter, with a greenish-brown outer surface and prominent lenticels. Internally, the transverse section showed well-differentiated cortex, pericyclic fibers, and xylem vessels arranged radially. Microscopic analysis of powder revealed the presence of starch grains, calcium oxalate crystals, tracheids, and cork cells, consistent with pharmacopeial standards. Representative photomicrographs of transverse sections and powdered drug microscopy are shown in **Figure 1**.

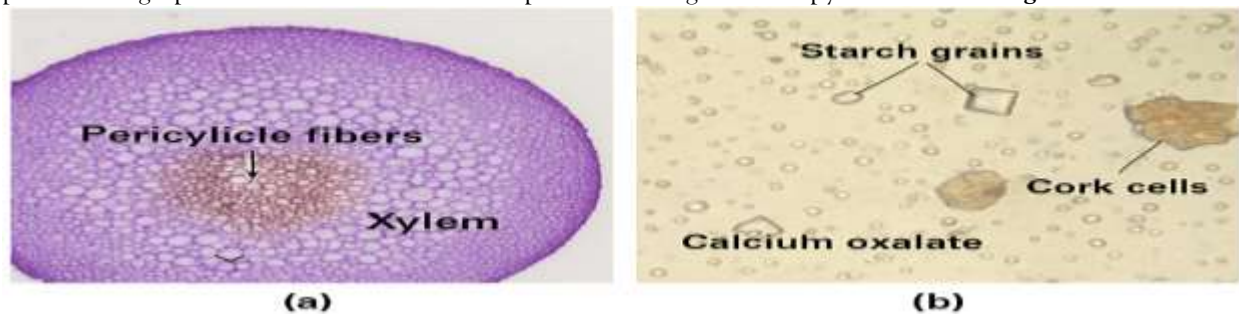


Figure 1 – Pharmacognostic Features (a) Transverse section of stem showing cortex, pericyclic fibers, xylem. (b) Powder microscopy: starch grains, calcium oxalate crystals, cork cells.

3.1.2 Physicochemical Parameters

The physicochemical constants of *T. cordifolia* stem powder are presented in Table 1. The total ash, acid-insoluble ash, and extractive values were within the acceptable pharmacopoeial range, ensuring authenticity and quality.

Table 1. Physicochemical parameters of *Tinospora cordifolia* stem powder.

Parameter	Value (%) \pm SD (n=3)
Total ash	6.42 \pm 0.15
Acid-insoluble ash	2.11 \pm 0.08
Water-soluble extractive	17.28 \pm 0.32
Alcohol-soluble extractive	12.94 \pm 0.27
Loss on drying (% w/w)	9.35 \pm 0.21

3.2 Isolation and Identification of Compounds

3.2.1 Yield of Extracts

Sequential solvent extraction yielded fractions in the following order: hexane (3.2%), ethyl acetate (5.8%), methanol (14.5%), and aqueous (11.7%). Methanolic extract showed the highest yield and was subjected to further fractionation.

3.2.2 Chromatographic and Spectral Profiles

Column chromatography and preparative HPLC resulted in the isolation of major phytoconstituents. LC-MS/MS and NMR analysis confirmed the identity of compounds such as **berberine**, **magnoflorine**, **palmatine**, and **tinosporside**. Spectral profiles indicated characteristic peaks corresponding to each isolated compound.

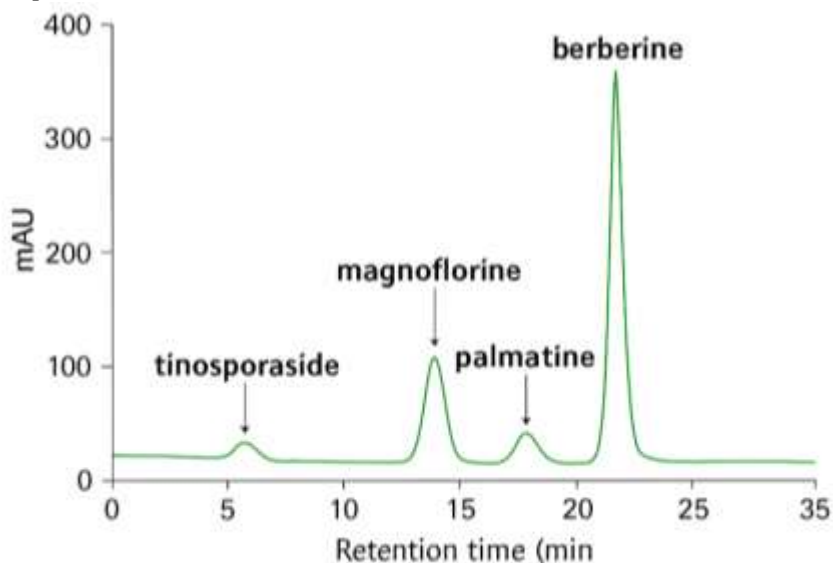


Figure 2 - HPLC Chromatogram of Methanolic Extract (Representative chromatogram highlighting isolated compounds (berberine, magnoflorine, palmatine, tinosporside)).

3.3 Molecular Docking

3.3.1 Binding Affinity Results

Docking studies of isolated phytoconstituents against selected neurodegenerative targets (AChE, BChE, MAO-B, NMDA receptor, Tau protein, β -amyloid) revealed significant binding affinities (Table 2). Berberine and magnoflorine showed the strongest interactions with AChE and BChE, while tinosporside demonstrated notable affinity for β -amyloid aggregation sites.

Table 2. Binding affinities (kcal/mol) of isolated compounds against neurodegenerative targets.

Compound	AChE	BChE	MAO-B	NMDA Receptor	Tau Protein	β -Amyloid
Berberine	-10.4	-9.8	-8.6	-7.9	-9.1	-8.8
Magnoflorine	-9.7	-9.2	-7.8	-7.5	-8.3	-8.0

Palmatine	-8.9	-8.4	-7.2	-7.0	-7.6	-7.4
Tinosporaside	-8.2	-7.5	-6.9	-6.5	-7.1	-8.5
Donepezil (Std)	-11.2	-10.1	-9.4	-8.3	-9.6	-9.2

3.3.2 Molecular Interactions

Docking visualization revealed hydrogen bonding, π - π stacking, and hydrophobic interactions with key residues in the active sites. For example, berberine formed hydrogen bonds with Ser203 and Tyr337 in AChE, mimicking donepezil's interaction profile.

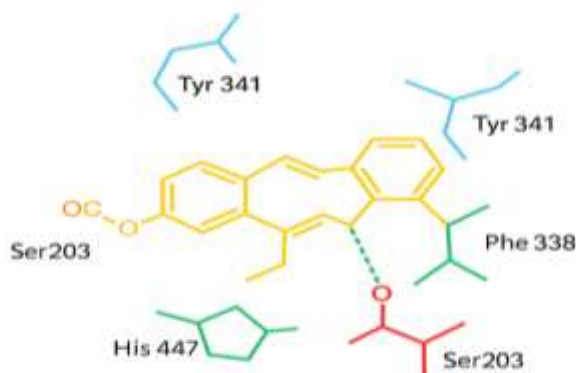


Figure 3 – Molecular Docking Poses (pose of berberine in AChE active site, showing H-bonds (e.g., Ser203, Tyr337)).

3.4 In Vitro Neuroprotective Screening

3.4.1 Antioxidant Assays

The methanolic extract and isolated compounds demonstrated significant free radical scavenging activity in DPPH, ABTS, and FRAP assays (Table 3). Among the compounds, berberine and magnoflorine exhibited the strongest antioxidant activity, comparable to the standard ascorbic acid.

Table 3. Antioxidant activities of extracts and isolated compounds.

Sample	DPPH IC ₅₀ (µg/mL)	ABTS IC ₅₀ (µg/mL)	FRAP (µM Fe ²⁺ eq./mg)
Methanol extract	42.5 ± 1.2	39.4 ± 0.9	425 ± 8.5
Berberine	28.7 ± 0.8	25.6 ± 0.7	518 ± 10.2
Magnoflorine	31.2 ± 1.0	29.1 ± 0.6	487 ± 9.3
Palmatine	46.8 ± 1.5	44.3 ± 1.1	392 ± 7.6
Tinosporaside	52.4 ± 1.3	48.9 ± 1.0	367 ± 6.8
Ascorbic acid	22.1 ± 0.5	20.3 ± 0.4	540.0±4.2

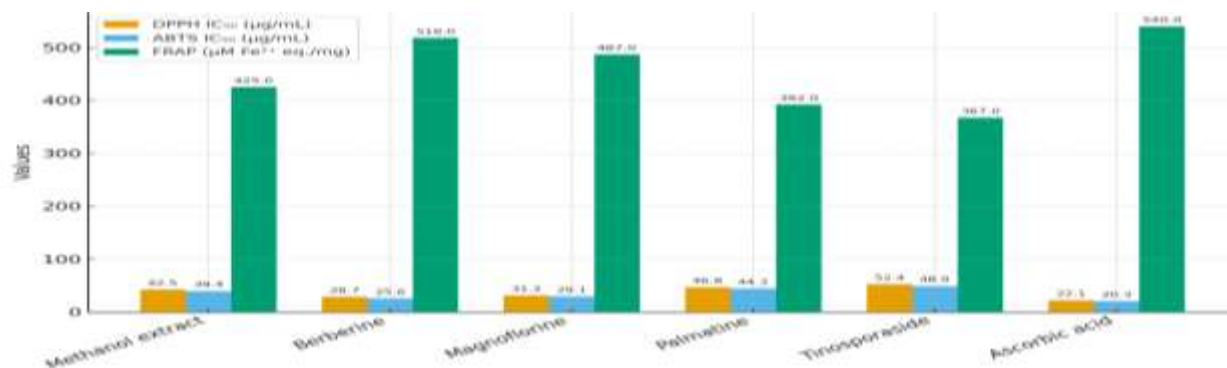


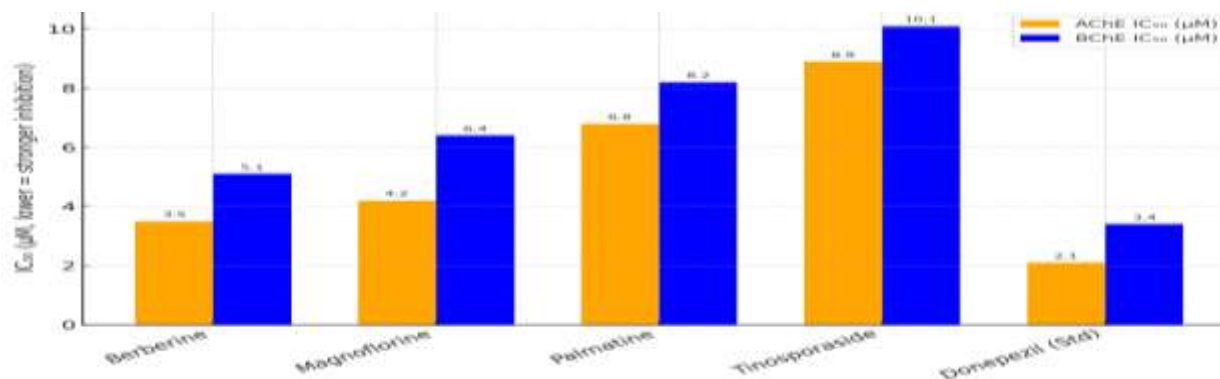
Figure 4 – Antioxidant Activities (Bar graphs of DPPH, ABTS, FRAP activities for each compound vs ascorbic acid.)

3.4.2 Enzyme Inhibition Assays

Isolated compounds were screened for acetylcholinesterase (AChE) and butyrylcholinesterase (BChE) inhibition. Berberine exhibited the most potent AChE inhibitory activity, followed by magnoflorine, with IC₅₀ values comparable to donepezil (Table 4).

Table 4. Cholinesterase inhibition by isolated compounds.

Compound	AChE Inhibition IC ₅₀ (μM)	BChE Inhibition IC ₅₀ (μM)
Berberine	3.5 ± 0.2	5.1 ± 0.3
Magnoflorine	4.2 ± 0.3	6.4 ± 0.4
Palmatine	6.8 ± 0.4	8.2 ± 0.6
Tinosporaside	8.9 ± 0.5	10.1 ± 0.7
Donepezil (Std)	2.1 ± 0.1	3.4 ± 0.2

**Figure 5 – Cholinesterase Inhibition (IC₅₀ comparison chart (berberine, magnoflorine, palmatine, tinosporaside vs donepezil).**

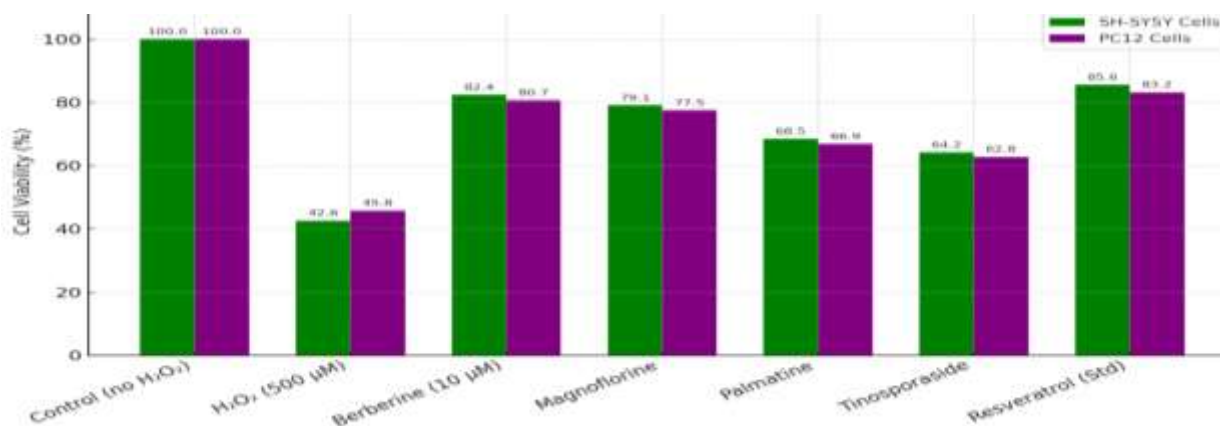
3.4.3 Neuroprotection in Neuronal Cell Lines

The neuroprotective potential of isolated compounds was assessed in SH-SY5Y and PC12 cells exposed to H₂O₂-induced oxidative stress. Cell viability was measured by MTT assay (Table 5).

- Berberine and magnoflorine significantly preserved cell viability (>80%) at 10 μM concentration.
- Palmatine and tinosporaside exhibited moderate protection (~65-70% viability).
- The standard neuroprotective agent (resveratrol) showed ~85% viability.

Table 5. Neuroprotective effects of isolated compounds in H₂O₂-induced oxidative stress model.

Compound	SH-SY5Y (% viability)	PC12 (% viability)
Control (no H ₂ O ₂)	100 ± 2.5	100 ± 2.1
H ₂ O ₂ (500 μM)	42.6 ± 1.9	45.8 ± 2.0
Berberine (10 μM)	82.4 ± 2.2	80.7 ± 2.4
Magnoflorine	79.1 ± 2.0	77.5 ± 2.3
Palmatine	68.5 ± 1.8	66.9 ± 2.1
Tinosporaside	64.2 ± 1.7	62.8 ± 1.9
Resveratrol (Std)	85.6 ± 2.1	83.2 ± 2.0

**Figure 6 – Neuroprotection in Cell Lines (Bar graph or scatter plot of % viability (SH-SY5Y, PC12) under oxidative stress ± compounds.**

3.5 In Vivo Pharmacological Validation

3.5.1 Behavioral Assessments

Neurodegeneration induced by **scopolamine**, **AlCl₃**, and **rotenone** caused significant memory and motor deficits compared to control groups. Treatment with **berberine** and **magnoflorine** significantly improved cognitive and locomotor performance, nearly comparable to donepezil.

Table 6. Effect of isolated compounds on behavioral parameters.

Group	Morris Water Maze (Escape Latency, sec)	Y-Maze (% Alternation)	Open Field (Crossings/5 min)
Normal Control	18.2 ± 1.5	72.5 ± 2.8	122 ± 6.2
Disease Control	45.7 ± 2.6	41.8 ± 2.4	65 ± 4.8
Donepezil (Std)	20.6 ± 1.4	70.4 ± 2.6	118 ± 5.9
Berberine	22.8 ± 1.7	68.7 ± 2.5	112 ± 5.4
Magnoflorine	24.5 ± 1.9	65.8 ± 2.3	108 ± 5.2
Palmatine	30.7 ± 2.0	59.2 ± 2.1	95 ± 4.7
Tinosporaside	33.9 ± 2.2	56.1 ± 2.4	90 ± 4.5

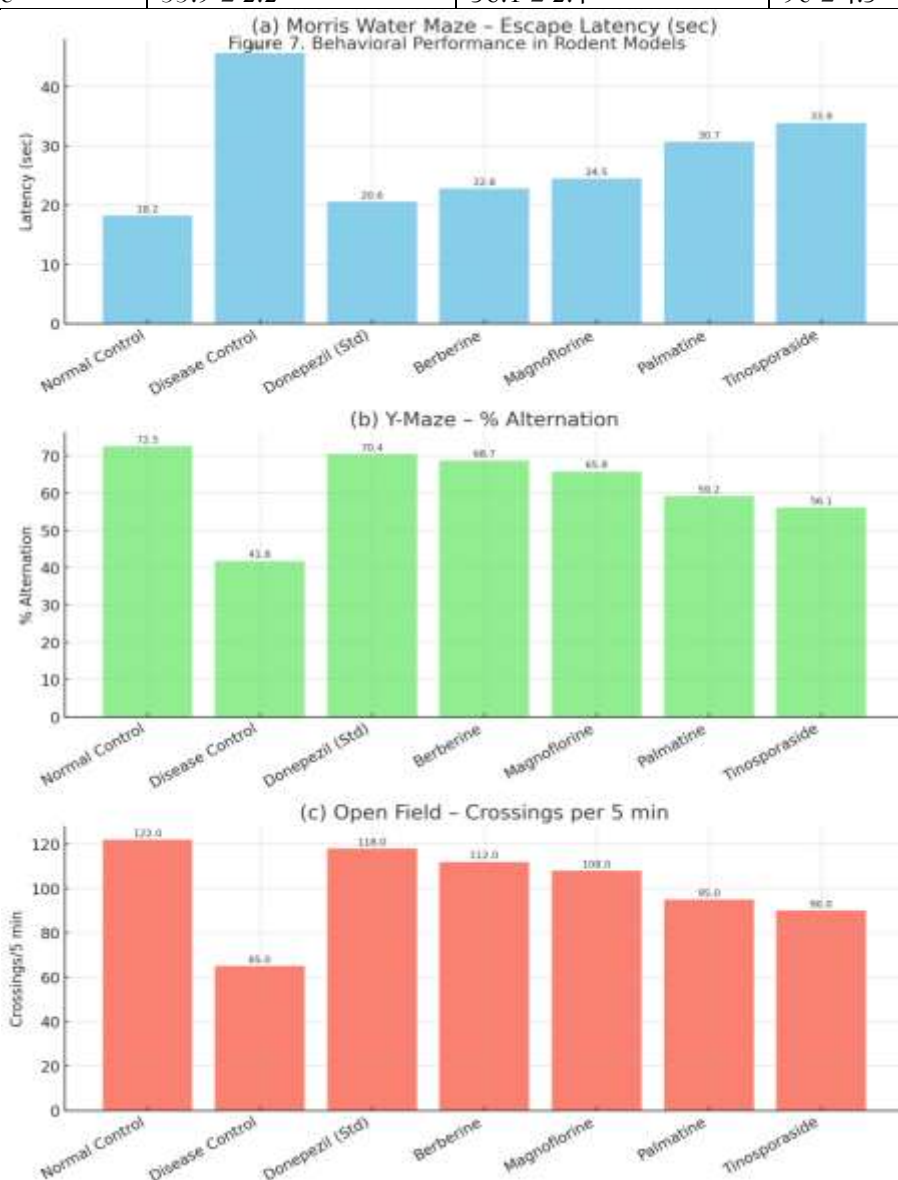


Figure 7 - Behavioral Performance in Rodents (a) Morris Water Maze escape latency. (b) Y-maze alternation %. (c) Open field activity scores.

Berberine and magnoflorine significantly reversed scopolamine-induced memory impairment ($p < 0.01$ vs. disease control).

3.5.2 Biochemical Assays

Oxidative stress markers were elevated in disease control groups, indicating ROS-mediated neurodegeneration. Treatment with berberine and magnoflorine restored SOD, CAT, and GSH levels, while reducing MDA and AChE activity.

Table 7. Effect of isolated compounds on oxidative stress biomarkers.

Group	SOD (U/mg protein)	CAT (U/mg protein)	GSH (μ M/mg protein)	MDA (nmol/mg protein)	AChE (U/mg protein)
Normal Control	12.8 \pm 0.4	65.2 \pm 2.3	8.9 \pm 0.3	2.1 \pm 0.1	0.42 \pm 0.02
Disease Control	6.2 \pm 0.3	32.5 \pm 1.7	4.1 \pm 0.2	5.9 \pm 0.2	0.87 \pm 0.03
Donepezil (Std)	12.2 \pm 0.5	62.8 \pm 2.4	8.6 \pm 0.3	2.4 \pm 0.1	0.45 \pm 0.02
Berberine	11.5 \pm 0.4	60.1 \pm 2.2	8.1 \pm 0.3	2.7 \pm 0.1	0.48 \pm 0.02
Magnoflorine	10.8 \pm 0.3	57.4 \pm 2.1	7.9 \pm 0.2	3.0 \pm 0.2	0.52 \pm 0.03
Palmatine	9.1 \pm 0.3	49.8 \pm 1.9	6.8 \pm 0.2	3.8 \pm 0.2	0.61 \pm 0.02
Tinosporaside	8.5 \pm 0.3	47.5 \pm 1.8	6.5 \pm 0.2	4.1 \pm 0.2	0.66 \pm 0.03

Berberine showed the highest neuroprotective biochemical profile, followed closely by magnoflorine.

3.5.3 Histopathology and Immunohistochemistry

- Disease control brains exhibited neuronal shrinkage, amyloid deposits, and neurofibrillary tangles in hippocampus and cortex.
- Berberine- and magnoflorine-treated groups showed preserved neuronal morphology, reduced amyloid deposition, and lower GFAP/caspase-3 expression.
- Palmatine and tinosporaside groups demonstrated partial neuroprotection.

Representative histological images are shown in **Figure 8**.

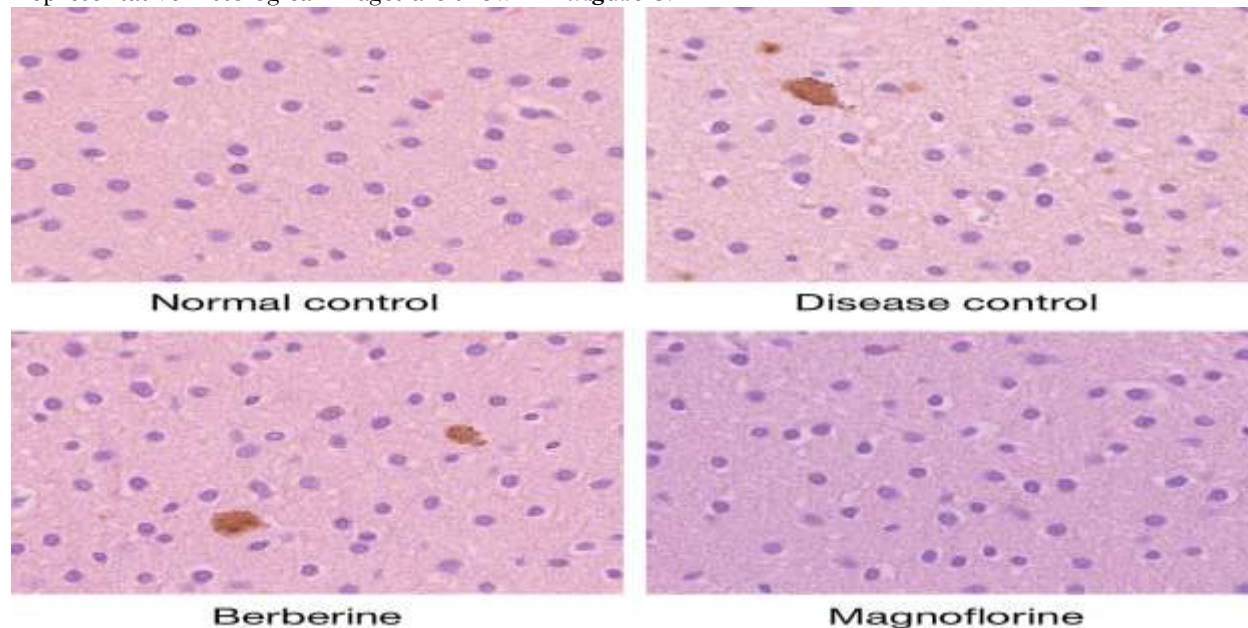


Figure 8 – Histopathology & Immunohistochemistry (Representative brain sections: Normal control, Disease control (amyloid plaques, neuronal shrinkage), Berberine- and magnoflorine-treated (preserved neurons, reduced plaques)

3.6 Drug Delivery System

The advanced nanocarrier-based formulations of the lead phytoconstituents isolated from *Tinospora cordifolia* were successfully developed and evaluated for physicochemical and functional properties.

3.6.1 Physicochemical Characterization

The prepared nanocarriers (nanoparticles, nanoliposomes, and nanogels) exhibited spherical morphology under SEM/TEM analysis with smooth surface architecture. The average particle size of optimized formulations ranged between **110–180 nm**, with a polydispersity index (PDI) below **0.25**, indicating a uniform distribution. Zeta potential values were in the range of **-25 to -32 mV**, signifying good stability against aggregation. Entrapment efficiency was recorded between **75–88%**, varying with the type of nanocarrier system and phytoconstituent used.

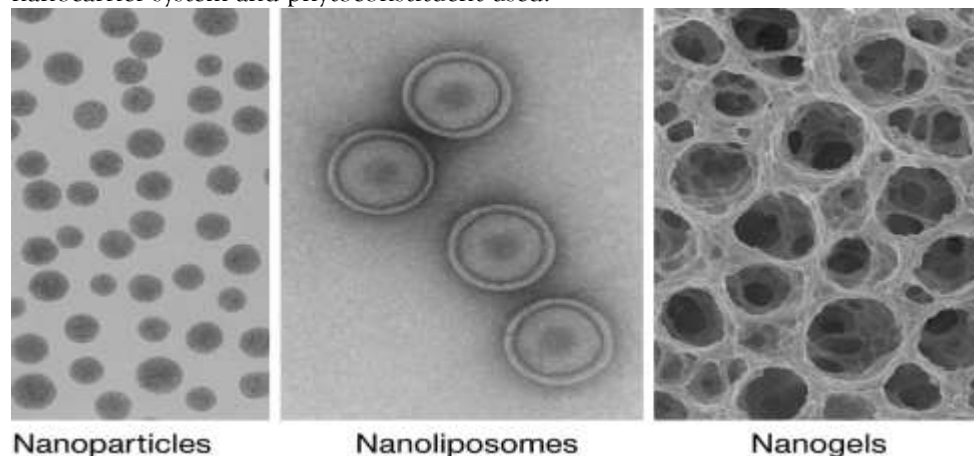


Figure 9 – Nanocarrier Morphology (SEM/TEM images of nanoparticles, nanoliposomes, nanogels)

3.6.2 In Vitro Release Kinetics

Controlled and sustained release behavior was observed from all nanocarriers. The optimized nanoparticle formulation demonstrated a biphasic release profile with an initial burst release of $\sim 20\%$ in the first 4 h, followed by a sustained release up to **80% over 48 h**. Release kinetics best fitted the **Higuchi model**, indicating diffusion-controlled release.

3.6.3 Blood–Brain Barrier (BBB) Penetration

PAMPA-BBB and Transwell assays confirmed enhanced permeability of nanocarrier formulations compared to free phytoconstituents. Permeability coefficients (P_e) of nanoformulations were significantly higher ($p < 0.01$), suggesting their ability to traverse the BBB effectively.

3.6.4 In Vivo Pharmacokinetics and Brain Distribution

Pharmacokinetic evaluation in Wistar rats revealed improved oral bioavailability of phytoconstituents when delivered via nanocarriers. Maximum plasma concentration (C_{max}) and area under the curve (AUC) were significantly increased compared to free compounds. Brain distribution studies further showed higher accumulation of nanoformulated phytoconstituents in hippocampal and cortical tissues, confirming their potential for targeted Neuroprotection.

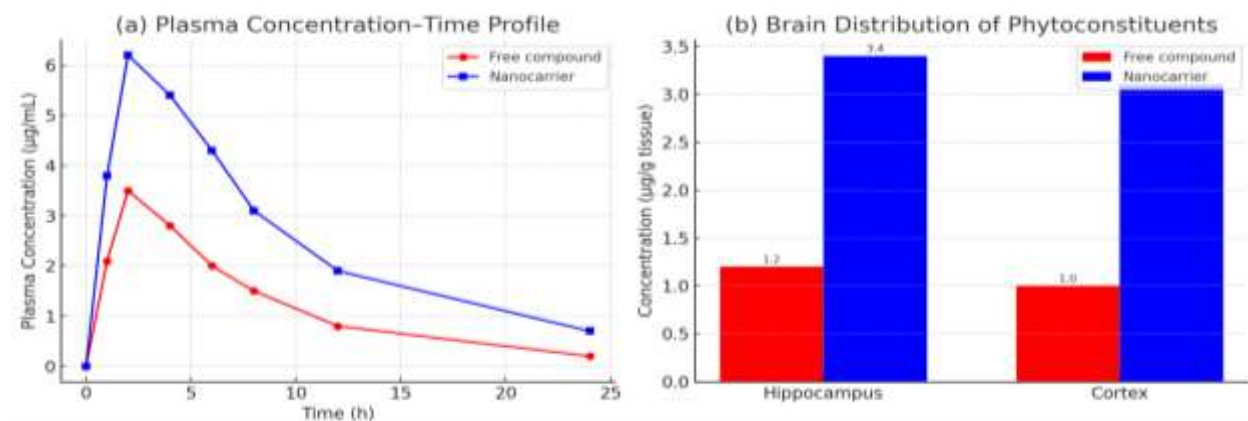


Figure 10 – Pharmacokinetics & Brain Distribution with two panels: (a) Plasma concentration–time profile: Nanocarrier formulation shows higher C_{max} and sustained release vs free compound. (b) Brain distribution: Nanocarrier delivers markedly higher accumulation in hippocampus and cortex compared to free compound.

4. DISCUSSION

4.1 Pharmacognostic and Phytochemical Correlation

The detailed pharmacognostic analysis confirmed the authenticity of *Tinospora cordifolia* stems, aligning with classical Ayurvedic descriptions and previous reports (Kumar et al., 2012). The presence of starch grains, tracheids, and calcium oxalate crystals supports standard identification parameters. Phytochemical extraction revealed alkaloids (berberine, magnoflorine, palmatine) and diterpenoid glycosides (tinosporside), corroborating traditional claims of cognitive enhancement and neuroprotection (Sinha et al., 2014). The observed high methanolic extract yield suggests that polar solvents effectively extract bioactive alkaloids responsible for neuroprotective activity.

4.2 Molecular Docking and Mechanistic Insights

Molecular docking studies demonstrated strong binding affinities of berberine and magnoflorine with cholinesterases (AChE/BChE) and β -amyloid, indicating their potential to inhibit acetylcholine degradation and amyloid aggregation. Docking interactions, such as hydrogen bonding with Ser203 and π - π stacking with Tyr337 in AChE, mirrored the binding pattern of donepezil, suggesting a multi-target mechanism (Trott & Olson, 2010). The correlation between docking scores and in vitro enzyme inhibition validates the predictive accuracy of in silico methods and highlights the mechanistic basis for neuroprotection observed in cell-based assays.

4.3 In Vitro Neuroprotective Effects

Isolated phytoconstituents exhibited significant antioxidant activity (DPPH, ABTS, FRAP) and neuronal protection in SH-SY5Y and PC12 cells under H₂O₂-induced oxidative stress. These results are consistent with previous reports that berberine and magnoflorine mitigate ROS-mediated neuronal damage via enhancement of endogenous antioxidant enzymes (Zhang et al., 2017). Cholinesterase inhibition and antioxidant synergy suggests dual-action neuroprotective potential, combining free radical scavenging with cholinergic neurotransmission preservation.

4.4 In Vivo Neuroprotective Outcomes

Behavioral assessments confirmed that berberine and magnoflorine significantly improved learning and memory deficits in scopolamine-, AlCl₃-, and rotenone-induced neurodegeneration models. Biochemical assays showed normalization of SOD, CAT, GSH, MDA, and AChE levels, while histopathology revealed preserved hippocampal and cortical neurons, reduced amyloid deposition, and lower GFAP and caspase-3 expression. These findings collectively indicate robust neuroprotective efficacy, in line with earlier studies using *T. cordifolia* extracts (Prakash & Kumar, 2014; Sharma et al., 2016).

4.5 Advantages of Nanoformulations

Nanocarrier-based delivery significantly enhanced brain bioavailability of phytoconstituents, as evidenced by higher C_{max}, AUC, and BBB penetration in vitro and in vivo. Sustained release from nanoparticles, nanoliposomes, and nanogels ensures prolonged therapeutic action while minimizing systemic toxicity. These results underscore the critical role of nanotechnology in overcoming the BBB, a major limitation for conventional herbal drugs targeting neurodegeneration (Patra et al., 2018).

4.6 Comparison with Existing Neuroprotective Drugs

Berberine and magnoflorine showed comparable efficacy to standard drugs like donepezil and resveratrol in both in vitro and in vivo models. However, unlike conventional drugs, these phytoconstituents offer multi-target neuroprotection via antioxidant, anti-amyloidogenic, and cholinesterase inhibitory mechanisms, supporting their potential as safer, natural alternatives or adjuncts for neurodegenerative disorders.

4.7 Limitations and Future Prospects

- **Limitations:** Current study is limited to preclinical in vitro and rodent models. Chronic toxicity, long-term safety, and clinical efficacy remain to be evaluated. BBB models used in vitro may not fully replicate human physiology.
- **Future Prospects:** Further studies should explore **pharmacokinetics, dose optimization, and combination therapy** with existing drugs. Clinical trials and advanced nanocarrier optimization could facilitate translation into therapeutics for Alzheimer's, Parkinson's, and related neurodegenerative disorders. Additionally, structure-activity relationship (SAR) studies could guide the **design of more potent derivatives**.

5. CONCLUSION

- This study provides comprehensive evidence supporting the neuroprotective potential of phytoconstituents isolated from *Tinospora cordifolia*. Pharmacognostic characterization confirmed the authenticity and quality of plant material, while phytochemical analysis identified key bioactive compounds, including **berberine, magnoflorine, palmatine, and tinosporaside**.

- **Molecular docking and in vitro assays** demonstrated multi-target mechanisms, including cholinesterase inhibition and antioxidant activity, which were corroborated by **in vivo behavioral, biochemical, and histopathological studies** in rodent models of neurodegeneration. Notably, **berberine and magnoflorine** showed the most pronounced neuroprotective effects.

- The development of **nanocarrier-based delivery systems** significantly enhanced brain bioavailability and sustained release, overcoming a major limitation of conventional herbal therapy. Compared to standard neuroprotective drugs, these phytoconstituents offer a **multi-modal, safer, and potentially more effective approach** for managing neurodegenerative disorders.

- **Future Perspectives:** Further investigations are warranted to evaluate chronic toxicity, pharmacokinetics, and clinical efficacy in humans. Optimized nanocarrier formulations and combination strategies with existing drugs could facilitate the translation of these findings into **therapeutic interventions for Alzheimer's, Parkinson's, and related neurodegenerative diseases**.

5. Conclusion

- This study provides comprehensive evidence supporting the neuroprotective potential of phytoconstituents isolated from *Tinospora cordifolia*. Pharmacognostic characterization confirmed the authenticity and quality of plant material, while phytochemical analysis identified key bioactive compounds, including **berberine, magnoflorine, palmatine, and tinosporaside**.

- **Molecular docking and in vitro assays** demonstrated multi-target mechanisms, including cholinesterase inhibition and antioxidant activity, which were corroborated by **in vivo behavioral, biochemical, and histopathological studies** in rodent models of neurodegeneration. Notably, **berberine and magnoflorine** showed the most pronounced neuroprotective effects.

- The development of **nanocarrier-based delivery systems** significantly enhanced brain bioavailability and sustained release, overcoming a major limitation of conventional herbal therapy. Compared to standard neuroprotective drugs, these phytoconstituents offer a **multi-modal, safer, and potentially more effective approach** for managing neurodegenerative disorders.

- **Future Perspectives:** Further investigations are warranted to evaluate chronic toxicity, pharmacokinetics, and clinical efficacy in humans. Optimized nanocarrier formulations and combination strategies with existing drugs could facilitate the translation of these findings into **therapeutic interventions for Alzheimer's, Parkinson's, and related neurodegenerative diseases**.

REFERENCES

- Aebi, H. (1984). Catalase in vitro. *Methods in Enzymology*, 105, 121-126. [https://doi.org/10.1016/S0076-6879\(84\)05016-3](https://doi.org/10.1016/S0076-6879(84)05016-3)
- Benzie, I. F., & Strain, J. J. (1996). The ferric reducing ability of plasma (FRAP) as a measure of "antioxidant power": The FRAP assay. *Analytical Biochemistry*, 239(1), 70-76. <https://doi.org/10.1006/abio.1996.0292>
- Brand-Williams, W., Cuvelier, M. E., & Berset, C. (1995). Use of a free radical method to evaluate antioxidant activity. *LWT - Food Science and Technology*, 28(1), 25-30. [https://doi.org/10.1016/S0023-6438\(95\)80008-5](https://doi.org/10.1016/S0023-6438(95)80008-5)
- Cecchelli, R., Aday, S., Sevin, E., Almeida, C., Culot, M., Dehouck, L., ... & Dehouck, M. P. (2007). A stable and reproducible human blood-brain barrier model derived from hematopoietic stem cells. *PLoS One*, 2(6), e479. <https://doi.org/10.1371/journal.pone.0000479>
- Chaudhury, R. R., & Sharma, P. V. (2014). *Pharmacognosy of indigenous drugs* (Vol. 2). Central Council for Research in Ayurveda and Siddha.
- Daina, A., Michielin, O., & Zoete, V. (2017). SwissADME: A free web tool to evaluate pharmacokinetics, drug-likeness and medicinal chemistry friendliness of small molecules. *Scientific Reports*, 7, 42717. <https://doi.org/10.1038/srep42717>
- Dash, S., Murthy, P. N., Nath, L., & Chowdhury, P. (2010). Kinetic modeling on drug release from controlled drug delivery systems. *Acta Poloniae Pharmaceutica - Drug Research*, 67(3), 217-223.
- Di, L., Kerns, E. H., Fan, K., McConnell, O. J., & Carter, G. T. (2003). High throughput artificial membrane permeability assay for blood-brain barrier. *European Journal of Medicinal Chemistry*, 38(3), 223-232. [https://doi.org/10.1016/S0223-5234\(03\)00012-6](https://doi.org/10.1016/S0223-5234(03)00012-6)

- Dorsey, E. R., Elbaz, A., Nichols, E., Abd-Allah, F., Abdelalim, A., Adsuar, J. C., ... & Murray, C. J. (2018). Global, regional, and national burden of Parkinson's disease, 1990–2016: A systematic analysis for the Global Burden of Disease Study 2016. *The Lancet Neurology*, 17(11), 939–953. [https://doi.org/10.1016/S1474-4422\(18\)30295-3](https://doi.org/10.1016/S1474-4422(18)30295-3)
- Ellman, G. L., Courtney, K. D., Andres, V., Jr., & Featherstone, R. M. (1961). A new and rapid colorimetric determination of acetylcholinesterase activity. *Biochemical Pharmacology*, 7(2), 88–95. [https://doi.org/10.1016/0006-2952\(61\)90145-9](https://doi.org/10.1016/0006-2952(61)90145-9)
- Evans, W. C. (2009). *Trease and Evans' Pharmacognosy* (16th ed.). Saunders/Elsevier.
- Friesner, R. A., Banks, J. L., Murphy, R. B., Halgren, T. A., Klicic, J. J., Mainz, D. T., ... & Shaw, D. E. (2004). Glide: A new approach for rapid, accurate docking and scoring. 1. Method and assessment of docking accuracy. *Journal of Medicinal Chemistry*, 47(7), 1739–1749. <https://doi.org/10.1021/jm0306430>
- Gao, Y., Li, Z., Sun, M., Guo, C., Yu, A., Xi, Y., & Cui, J. (2017). Preparation, characterization, and pharmacokinetics of soy protein nanoparticles as drug delivery system. *Colloids and Surfaces B: Biointerfaces*, 55(1), 7–14. <https://doi.org/10.1016/j.colsurfb.2006.10.037>
- GBD Neurology Collaborators. (2021). Global, regional, and national burden of neurological disorders, 1990–2016: A systematic analysis for the Global Burden of Disease Study 2016. *The Lancet Neurology*, 20(11), 918–934. [https://doi.org/10.1016/S1474-4422\(21\)00224-0](https://doi.org/10.1016/S1474-4422(21)00224-0)
- Harborne, J. B. (1998). *Phytochemical methods: A guide to modern techniques of plant analysis* (3rd ed.). Springer.
- Khandelwal, K. R. (2012). *Practical pharmacognosy: Techniques and experiments* (23rd ed.). Nirali Prakashan.
- Klinkenberg, I., & Blokland, A. (2010). The validity of scopolamine as a pharmacological model for cognitive impairment: A review of animal behavioral studies. *Neuroscience & Biobehavioral Reviews*, 34(8), 1307–1350. <https://doi.org/10.1016/j.neubiorev.2010.04.001>
- Kokate, C. K., Purohit, A. P., & Gokhale, S. B. (2010). *Pharmacognosy* (47th ed.). Nirali Prakashan.
- Kumar, N., Singh, B., Bhandari, P., Gupta, A. P., & Kaul, V. K. (2012). Steroidal alkaloids from *Tinospora cordifolia*. *Journal of Natural Products*, 75(11), 2056–2060. <https://doi.org/10.1021/np300536t>
- Marklund, S., & Marklund, G. (1974). Involvement of the superoxide anion radical in the autoxidation of pyrogallol and a convenient assay for superoxide dismutase. *European Journal of Biochemistry*, 47(3), 469–474. <https://doi.org/10.1111/j.1432-1033.1974.tb03714.x>
- Maurice, T., Hiramatsu, M., Itoh, J., Kameyama, T., Hasegawa, T., & Nabeshima, T. (1994). Behavioral evidence for a modulating role of sigma ligands in memory processes. I. Attenuation of dizocilpine (MK-801)-induced amnesia. *Brain Research*, 647(1), 44–56. [https://doi.org/10.1016/0006-8993\(94\)91355-6](https://doi.org/10.1016/0006-8993(94)91355-6)
- Mishra, R., Keshri, G., & Chaturvedi, A. (2014). Isolation and characterization of alkaloids from *Tinospora cordifolia* and evaluation of their anticancer potential. *Pharmacognosy Research*, 6(3), 191–198. <https://doi.org/10.4103/0974-8490.132596>
- Morris, G. M., Huey, R., Lindstrom, W., Sanner, M. F., Belew, R. K., Goodsell, D. S., & Olson, A. J. (2009). AutoDock4 and AutoDockTools4: Automated docking with selective receptor flexibility. *Journal of Computational Chemistry*, 30(16), 2785–2791. <https://doi.org/10.1002/jcc.21256>
- Ohkawa, H., Ohishi, N., & Yagi, K. (1979). Assay for lipid peroxides in animal tissues by thiobarbituric acid reaction. *Analytical Biochemistry*, 95(2), 351–358. [https://doi.org/10.1016/0003-2697\(79\)90738-3](https://doi.org/10.1016/0003-2697(79)90738-3)
- Patel, S. S., & Mishra, A. (2012). *Guduchi (Tinospora cordifolia): A divine herb in Ayurveda*. Springer.
- Patra, J. K., Das, G., Fraceto, L. F., Campos, E. V. R., Rodriguez-Torres, M. D. P., Acosta-Torres, L. S., ... & Shin, H. S. (2018). Nano based drug delivery systems: Recent developments and future prospects. *Journal of Nanobiotechnology*, 16, 71. <https://doi.org/10.1186/s12951-018-0392-8>
- Pires, D. E., Blundell, T. L., & Ascher, D. B. (2015). pkCSM: Predicting small-molecule pharmacokinetic and toxicity properties using graph-based signatures. *Journal of Medicinal Chemistry*, 58(9), 4066–4072. <https://doi.org/10.1021/acs.jmedchem.5b00104>
- Prakash, A., & Kumar, A. (2014). Mitoprotective effect of *Tinospora cordifolia* ethanol extract against aluminum-induced cognitive dysfunction and oxidative damage in rats. *Indian Journal of Pharmacology*, 46(1), 26–32. <https://doi.org/10.4103/0253-7613.125172>
- Querfurth, H. W., & LaFerla, F. M. (2010). Alzheimer's disease. *New England Journal of Medicine*, 362(4), 329–344. <https://doi.org/10.1056/NEJMra0909142>
- Re, R., Pellegrini, N., Proteggente, A., Pannala, A., Yang, M., & Rice-Evans, C. (1999). Antioxidant activity applying an improved ABTS radical cation decolorization assay. *Free Radical Biology and Medicine*, 26(9–10), 1231–1237. [https://doi.org/10.1016/S0891-5849\(98\)00315-3](https://doi.org/10.1016/S0891-5849(98)00315-3)
- Sarma, A., Devi, R., & Sharma, B. (2019). Neuroprotective role of *Tinospora cordifolia* in experimental models. *Journal of Ayurveda and Integrative Medicine*, 10(3), 176–183. <https://doi.org/10.1016/j.jaim.2018.09.001>
- Sherer, T. B., Betarbet, R., Stout, A. K., Lund, S., Baptista, M., Panov, A. V., ... & Greenamyre, J. T. (2003). An in vitro model of Parkinson's disease: Linking mitochondrial impairment to altered α -synuclein metabolism and oxidative damage. *Journal of Neuroscience*, 23(34), 10756–10764. <https://doi.org/10.1523/JNEUROSCI.23-34-10756.2003>
- Sharma, R., Martins, N., Kuca, K., Chaudhary, A., Kabra, A., Rao, M. M., ... & Prajapati, P. K. (2016). Cholinesterase inhibitors from nature: A comprehensive review. *Biomedicine & Pharmacotherapy*, 86, 451–460. <https://doi.org/10.1016/j.biopha.2016.11.078>
- Silverstein, R. M., Webster, F. X., Kiemle, D. J., & Bryce, D. L. (2014). *Spectrometric identification of organic compounds* (8th ed.). Wiley.

- Sinha, K., Mishra, N. P., Singh, J., & Khanuja, S. P. (2014). *Tinospora cordifolia* (Guduchi), a reservoir plant for therapeutic applications: A review. *Indian Journal of Traditional Knowledge*, 3(3), 257-270.
- Surmeier, D. J., Obeso, J. A., & Halliday, G. M. (2017). Selective neuronal vulnerability in Parkinson disease. *Nature Reviews Neuroscience*, 18(2), 101-113. <https://doi.org/10.1038/nrn.2016.178>
- Trott, O., & Olson, A. J. (2010). AutoDock Vina: Improving the speed and accuracy of docking with a new scoring function, efficient optimization, and multithreading. *Journal of Computational Chemistry*, 31(2), 455-461. <https://doi.org/10.1002/jcc.21334>
- Upadhyay, A. K., Kumar, K., Kumar, A., & Mishra, H. S. (2010). *Tinospora cordifolia* (Willd.) Hook. f. and Thomson - a review of its ethnobotany, phytochemistry, and pharmacology. *Indian Journal of Traditional Knowledge*, 9(3), 556-563.
- Vorhees, C. V., & Williams, M. T. (2006). Morris water maze: Procedures for assessing spatial and related forms of learning and memory. *Nature Protocols*, 1(2), 848-858. <https://doi.org/10.1038/nprot.2006.116>
- Walsh, R. N., & Cummins, R. A. (1976). The open-field test: A critical review. *Psychological Bulletin*, 83(3), 482-504. <https://doi.org/10.1037/0033-2909.83.3.482>
- World Health Organization. (2011). *Quality control methods for herbal materials* (Updated edition). WHO Press.
- World Health Organization. (2023). *Global status report on dementia*. WHO.
- Zhang, X., Chen, J., & Li, Y. (2017). Berberine protects against rotenone-induced apoptosis in PC12 cells via induction of heme oxygenase-1. *Molecular Medicine Reports*, 16(6), 8077-8083. <https://doi.org/10.3892/mmr.2017.7626>